Novel Image Alignment Technique for Extraction of Astrometry and Photometry from Small Field of View Astronomical Sensors.

Calum Meredith, Grant Privett, Simon George, Will Feline
Defence Science and Technology Laboratory, UK

ABSTRACT

In this study, we considered a situation where, using amateur-class commercial off-the-shelf (COTS) equipment, high angular resolution was deemed to be more important than use of a wide Field of View (FOV) in fixed-stare Geostationary Orbit (GEO) tracking. Due to the reduction in FOV to acquire the angular resolution, issues are often encountered in plate-solving the resulting imagery due to the reduced number of reference stars contained within the field. In this paper, we describe a novel image alignment technique that was developed by the Defence Science and Technology Laboratory (Dstl) to enable accurate astrometry to be derived from a sequence of images that, individually, could not be plate-solved due to a scarcity of background stars.

This new technique was used experimentally during the PHANTOM ECHOES 2 experiment to obtain absolute astrometric data on Intelsat 10-02 and Mission Extension Vehicle-2 (MEV-2) during close-proximity manoeuvring: this was performed through conversion of simple (x, y) pixel space coordinates into a World Coordinate System (WCS) solution, as well as the generation of Gaia *G* equivalent determinations of photometric magnitude. While both results were of reduced astrometric and photometric accuracy from what might have been acquired by using a wide FOV sensor, the results were sufficient for tracking of GEO objects in proximity when supplied to Orbit Determination software. This approach allowed relatively inexpensive, small FOV, COTS equipment to contribute accurate astrometric and photometric data to the PHANTOM ECHOES 2 experiment.

1. INTRODUCTION

The costs of establishing multiple, longitudinally-dispersed Space Domain Awareness (SDA) systems can be high but they provide information that can enhance SDA beyond systems located only in one geographic location. To realise these benefits, lower-cost options can be considered, including the use of modest, relatively inexpensive commercial off-the-shelf (COTS) astronomical sensors. There is a need to understand the trade-off required to provide more affordable SDA capability by exploiting the ever increasing range of consumer level optical imagers and sensors now available: smaller, lower-cost optics and sensors can be versatile and easily-distributable within SDA tracking networks focussed on the surveillance and tracking of Geostationary Earth Orbit (GEO), but can have limitations in terms of field-of-view (FOV), non-optimal spatial resolution or poor tracking accuracy.

Typically when astronomical sensors are used for tracking objects at GEO, and often for other observation applications, the stars which are present in the background field are used as reference points to plate-solve each individual image frame and to determine the real-world coordinates for any given pixel in a frame. This requires a sufficient number of background stars to be available to compare with reference databases (such as the Sloan Digital Sky Survey [1], Two-Micron All-Sky Survey [2] and others) and, typically, a higher number of stars increases the likelihood of a successful match. A number of algorithms are available to provide this function, including Astrometry.net [3] which supports fully blind plate-solving. Having plate-solved these images, it is then possible to use these same stars, now identified, to compare with a reference database containing an estimate of their photometric parameters (such as Gaia DR2 [4]). This allows the brightness of targets across the entire frame to be calibrated on a magnitude scale. In this way, the frame can be both astrometrically and photometrically solved and the resulting data used for effective SDA.

However, for instruments with a narrow FOV, it may often be the case that too few background stars are found in the frame to enable plate-solving. Consequently, it becomes non-trivial to provide the automatic derivation of astrometric and calibrated photometric data. The examination of potential techniques to automatically and robustly calibrate frames (both astrometrically and photometrically) has been the focus of a recent study aligned with the PHANTOM ECHOES experiment [5, 6].

2. OBSERVATION CAMPAIGN

Between February and April 2021, the MEV-2 conducted rendezvous and docking with Intelsat 10-02, and was the subject of a coordinated experiment, known as PHANTOM ECHOES 2, exploring options to improve allied capabilities for protection of spacecraft in GEO: this experiment was previously reported at AMOS 2021 [6].

The PHANTOM ECHOES 2 experiment involved defence science and technology (S&T) agencies of the Five-Eyes (FVEY) nations – the United Kingdom, United States, Australia, Canada and New Zealand – to exploit this opportunity and to successfully pursue a coordinated SDA experiment, observing and scrutinising the dynamics and behaviours of the two satellites using a variety of ground- and space-based sensors.

During the observation campaign, the Defence Science and Technology Laboratory (Dstl) undertook an initiative to acquire data from UK amateur astronomers via a collaboration with Basingstoke Astronomical Society, under a continuation of the ARGUS project [7]. During the original ARGUS project, Dstl and Citizen Science astronomers collected observations of low-Earth orbit (LEO) satellites to examining the potential utility of employing a distributed array of amateur-class astronomical imaging systems. During the PHANTOM ECHOES 2 experiment, this was extended to the GEO environment, acquiring optical tracking data on Intelsat 10-02 and MEV-2. The ARGUS project astronomical sensors were joined by observations made by Dstl personnel using similar equipment collecting data over the same timeframe of the same satellites.

The instruments involved in the experiment are described in Table 1. They cover a range of FOVs but a number of the ARGUS sensors include FOVs that are narrow.

Table 1 – A summary of the instruments used during the study

Observer	Type / Description	Aperture / cm	FOV Size / deg	Pixel scale / "/px
1	TS-Optics 10" Ritchey-Chrétien astrograph, QSI 683wsg-8 CCD, iOptron CEM60-EC mount	25.4	0.515 × 0.388	0.558
2	Takahashi Mewlon 180C Dall-Kirkham reflector, SX Ultrastar Colour CCD, Takahashi EM-200 mount	18	0.240 × 0.180	0.31
3	Meade LX200 Schmidt-Cassegrain telescope, ZWO ASI294MC Pro CCD, iOptron CEM120 equatorial mount	35.6	0.248 × 0.169	0.427
4 (Dstl)	Sky-Watcher 114mm f/5 reflector, Sky-Watcher NEQ6 mount, Starlight Xpress Lodestar”	11.4	0.758 × 0.584	3.6

The collected dataset comprised of numerous, long image sequences (a total of 126 GB of data; typically comprising of more than 1000 frames per night from each telescope) taken with small FOV sensors with good spatial resolutions. In addition, the observations by Dstl provided 23 GB of data.

Across all of these datasets, to ensure that Intelsat 10-02 remained within frame, observations were undertaken without sidereal tracking, which caused the background stars to appear as streaks/trails. In this case, Intelsat 10-02 appeared as a circular source; likewise, when proximate, MEV-2 appeared in a similar way. Frequently, other GEO satellites in adjacent orbits could be observed in the data, including the THOR5, THOR6 and THOR7 spacecraft. Example images from this combined dataset are shown in Fig. 1, from two different instruments.

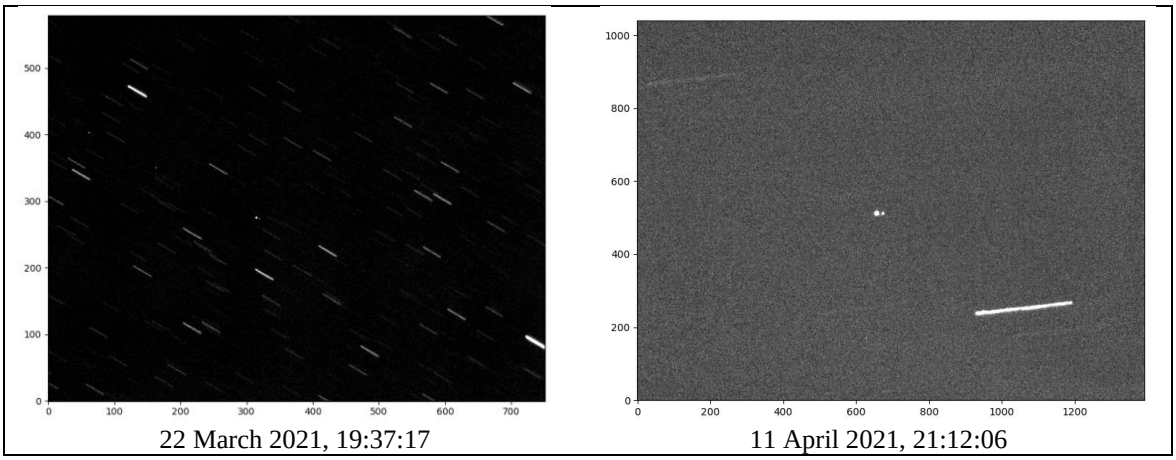

Fig. 1 – (Left) an image frame from the Dstl Observatory where stars are shown as streaks/trails and satellites appear as circular sources. The satellite left of centre of the frame is Intelsat 10-02 with a number of the THOR satellites towards the upper left of image. pixels **(Right)** an image frame from an ARGUS participant which features a narrower FOV and where it is possible to observe both Intelsat 10-02 and MEV-2 at the centre of the frame. The streaks/trails present in the frame arise from stars, but these are seen less frequently. In both images the axes display the pixel number to demonstrate the resolution and extent of the images.

3. DATA PROCESSING PIPELINE

The fundamentals of the data processing pipeline used by Dstl for optical telescope imagery have been reported at AMOS previously [7, 8], although the core capability has evolved in recent years to allow for imagery of GEO satellites, captured in fixed stare mode, to be processed. In the current pipeline, this is principally performed by first categorising sources as either stars or satellites by considering their ensemble median elongation (as shown in Fig. 1): in fixed pointing imagery, GEO satellites typically appear as circular sources, whilst stars create elongated trails. The derived pixel locations of satellites of interest are stored for later use, whilst the pixel location of the centroid of the star trails are supplied to the plate-solving algorithm [3] for astrometric solving. Once a World Coordinate System (WCS) has been found which links pixel coordinates to real-world sky coordinates, the derived satellite pixel locations can be used to determine their sky positions for provision to orbit determination software (for example, Dstl's Mission Planner software).

A major recent addition to the existing data processing pipeline has been to incorporate an ability to photometrically calibrate image frames and derive estimates of the visible magnitude of the satellite under observation. This calibration process aids in the production of light curves, and enables comparisons to be made with observations made by other instruments: this was used to good effect to support the broader PHANTOM ECHOES 2 experiment, by allowing comparisons of Dstl and ARGUS data with lightcurve data collected by other instruments. The processing pipeline used outputs from the plate-solving process to interrogate the Gaia DR [4] reference database, comparing instrumental flux with Gaia *G* equivalent determinations of photometric magnitude as reported by the database. Using an average of non-saturated stars, an estimate of this calibration can then be used to derive visible magnitudes for the target satellites observed in the data.

For much data, including that from the Dstl observatory, this software pipeline correctly used background stars to derive astrometry and photometry. However, for the data collected with a narrow FOV, when analysed, it was found that it was not often possible to yield an astrometric solution due to the reduced number of background stars captured. This difference is visible in Fig. 1 where the number of stars in the background of the two images is significantly different – for example, Astrometry.NET generally requires 8 or more stars in a frame as a minimum, and 20+ for accuracy. For these observations relative motion and photometry could be readily derived, but absolute values for the positions and the visual magnitudes of the satellites of interest could not be determined. As a result, it was necessary to develop and apply a novel processing technique to this dataset in order to acquire this information.

4. NOVEL IMAGE ALIGNMENT TECHNIQUE

With typical datasets consisting of ~1000 images per night collected at regular intervals, it is possible to consider the data as a time-series. Comparing one image frame with the subsequent one by eye, it is possible to identify stars in the background field of each that correspond to the same star, simply shifted by the relative sidereal motion of the sky between frames and any other sources of movement, including that of the telescope. Through inspection of the stars' pixel locations in the frame, it is possible to determine the translational offset between the two images (*dx*, *dy*) in the *x* and *y* axes. However, this manual approach is labour-intensive and an automatic process was developed.

Phase correlation is a method of determining the pixel translational offset between two images automatically, and has been used previously to solve many different image registration tasks [9, 10]. It relies on the principal that the two-dimensional Fourier transform of identical images (i_a, i_b), with one translationally shifted, will be identical in magnitude but with a phase shift that is related to the translational offset. The phase shift can be determined by calculating the cross-power spectrum (CPS) of the two images:

$$CPS = \frac{I_a \cdot I_b^*}{|I_a \cdot I_b^*|}$$

where I_a and I_b are the two dimensional Fourier transforms of i_a and i_b respectively. The inverse Fourier transform of the CPS then provides a two-dimensional array where pixel location of the peak magnitude, traditionally, is the translational offset between the two images. More complex variations of this algorithm exist to provide transforms for rotation and scale-invariances between images (as described in [11]) and these have been incorporated into Python libraries for general utility. One such library is imreg_dft, which was used in this study [12].

One challenge that is encountered when applying classic phase correlation to this dataset is that there are potentially two different offsets which the phase correlation may identify as 'correct': that of the background stars, and that of the satellites in the foreground. Which of these is identified as the principal translation can depend on how many stars are present in the images relative to satellites. To ensure robustness, a weighting function was used that allows for an initial guess at a translation to be favoured (within a Gaussian window). This was possible because, to a first approximation, the motion between two frames can be determined to the relative sidereal motion of the stars. It is possible to estimate this by considering the exposure time of the frames, the time between acquisition and an understanding of the instrument itself. Without knowledge of the initial pointing of the instrument, however, only a magnitude translation could be provided. For robustness, when this method was applied to longer datasets, considered as a time-series, this weighting could be constrained by an initial manual guess which was then updated by the most recently determined offset.

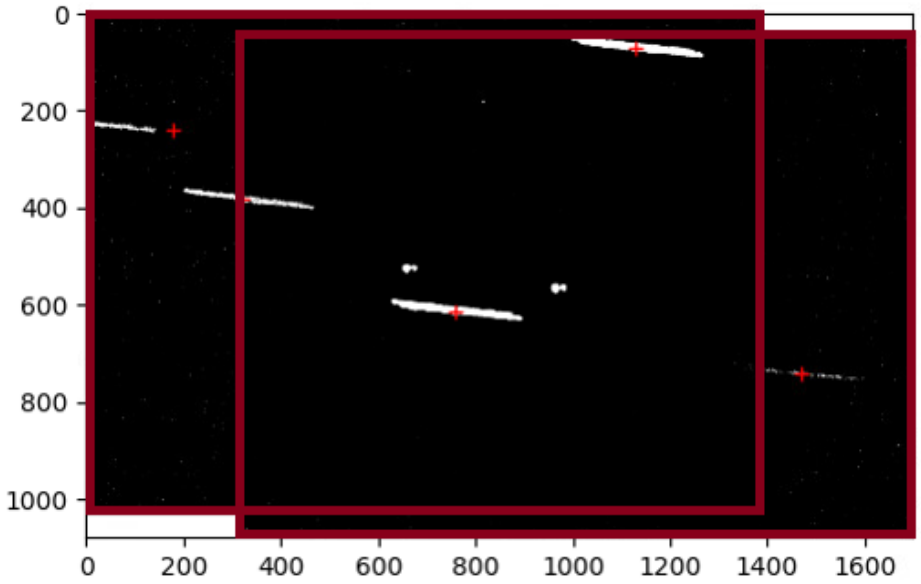

Fig. 2 – A combination of two image frames, each individual one similar to that found in Fig. 1 (right). Stars are identified as streaks/trails and the Intelsat 10-02 and MEV-2 pairing (circular objects) appears twice (translated). Red crosses indicate the centroid of detected stars.

Having determined this offset, the two images can then be aligned and combined (through co-addition) into a single, larger image. This is shown in Fig. 2, where three stars can be identified as featuring in both individual images. As described above, these common features have been used to determine the translational offset between the two images. The group of satellites (Intelsat 10-02 and MEV-2) now appear twice in a translated fashion as a side effect of aligning stars. By extending the image in this way, it is possible to see that the stars present in a single image gain an improved signal-to-noise ratio (SNR), and are now supplemented with a number of additional features (stars) which allow for better performance of the plate-solving process. Unfortunately, for sensors with this FOV, these algorithms generally require a greater number of stars than a simple combination of two images can deliver. The approach is therefore extended arbitrarily to N number of image frames, where N is a large enough number to generate a combined image with enough stars for plate-solving algorithms to solve. The exact value of N will depend on the instrument and observational details such as the galactic latitude of the FOV that is being sampled.

Fig. 3 (top) depicts an extension to 50 image frames, detecting ~24 stars (indicated by red crosses). Fig. 3 (bottom) provides an expanded section for easier visibility of smaller features. By co-adding these aligned images, this additionally provides the advantage of improving SNR by enhancing the visibility of coherent features (stars) and reducing incoherent noise. This also allows additional background stars that were near the image edge or of lower intensity in individual images, and not hence separable from noise, to be used by the plate-solving algorithm.

Pixel positions of the background stars are then extracted using a traditional clumping approach (as described in [7, 8]; although matched filtering and other techniques would be equally applicable) and supplied to an Astrometry.net installation to plate-solve the pixel space of the entire extended mosaic and derive the associated WCS transformations. Experimentally, it was found that altering the default Astrometry.net parameters to allow for solutions that were less constrained by star location accuracy aided in finding solutions from the stars extracted from these combined images. This is likely due to some remaining uncertainty in alignment between the images caused by field distortions. This may increase the likelihood of an inaccurate plate-solved solution but this did not appear to be significant in this study. It is possible to estimate the error in the plate-solved solution by calculating the median angular offset between the position of stars as provided by the whole image WCS transform and the known star location in the reference database.

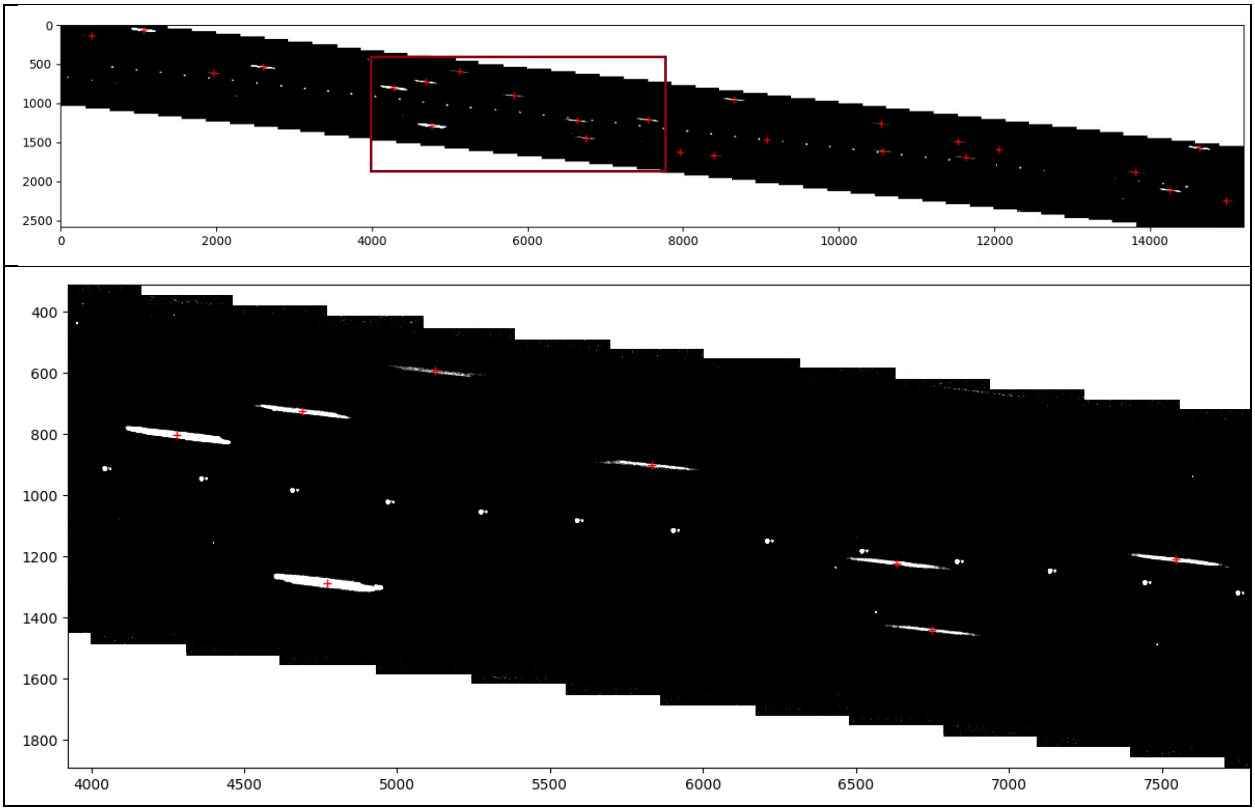

Fig. 3 – (top) the image alignment and combination process as applied to 50 image frames, with stars visible as streaks/trails and the grouping of satellites as regular circular features. **(bottom)** an extract of identical data (as shown by red box) to allow for small detail to be made visible.

From the WCS transformation acquired from Astrometry.net for the combined image, a subset WCS transformation could be assigned for each of the individual images. This allowed for the individual images to be used by subsequent processes that were not dependent on any knowledge of the generation process.

5. RESULTS

This technique enabled us to obtain absolute astrometric data on Intelsat 10-02 and MEV-2 during close-proximity manoeuvring, by using the detected pixel-space (x, y) coordinates of star trails from several image frames to determine a WCS transform. This allowed for the pixel locations of the satellites to be transformed into right ascension and declination coordinates, on a frame by frame basis. An example of positions derived from this process for Intelsat 10-02 and MEV-2 is shown in Fig. 4. Estimated errors associated with the WCS solution are also indicated. This demonstrates that real world tracked positions of satellites can be derived from these narrow FOV instruments where previously this was non-trivial.

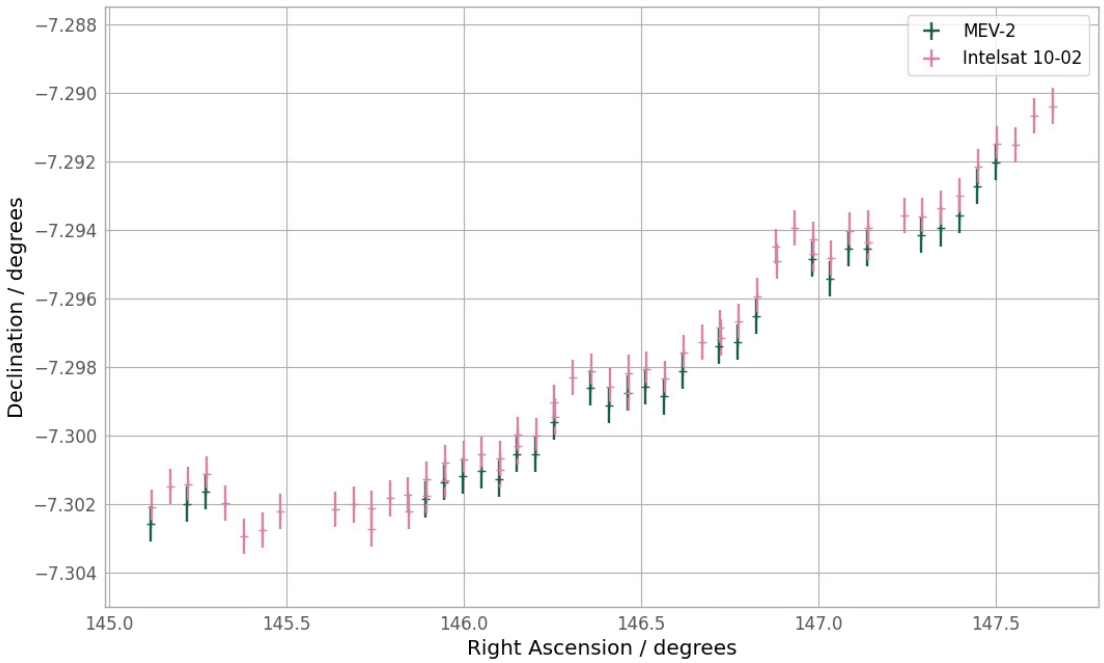

Fig. 4 – A plot of the on-sky position of MEV-2 (blue crosses) and Intelsat 10-02 (red crosses). The size of the bars of the cross indicates the calculated average error estimate.

In addition, this process enabled the generation of Gaia *G* equivalent determinations of photometric magnitudes FOV and allowed the production of calibrated light curves. This is caveated in that by its nature, for single frames, fewer stars were available for comparison with the reference database and taking one magnitude zero point (Z_p) across the combined time-series likely leads to reduced accuracy. Varying sky transparency (for example, due to thin cloud) over a course of combined observations would also reduce the accuracy of the estimated photometric magnitudes. It is possible that some of these inaccuracies could possibly be corrected for by, for example, considering the varying air mass. An example of this is shown in Fig. 5; the figure also shows some of the variability associated with such an approach, some of which is likely related to the reduced accuracy described. An estimate of the median error associated with Z_p can be calculated by comparison of the calculated magnitudes versus those of the reference database; this is also indicated in Fig. 5. However, where resolvable, the magnitude of MEV-2 was found to be significantly fainter than Intelsat 10-02, which was found to be consistent with other data and comparable to data available from contemporary sources such as data from the Warwick telescope [6].

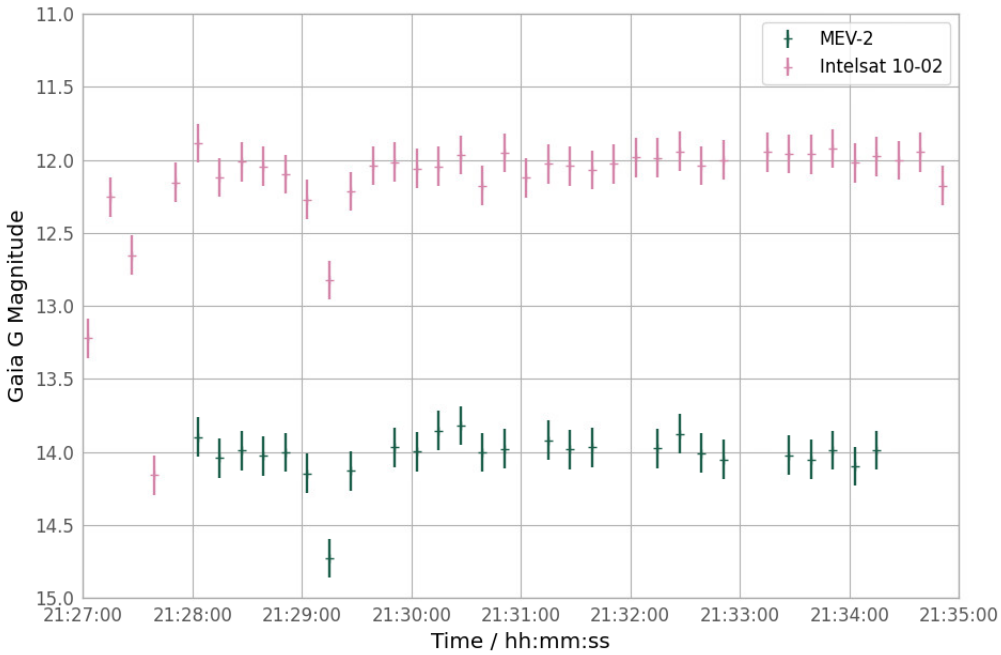

Fig. 5 – A plot of the determined Gaia *G* magnitude for Intelsat (red) and MEV-2 (blue). The size of the bars of the cross indicates the calculated average error estimate.

6. CONCLUSIONS

Whilst of lower accuracy than achievable with expensive wide FOV optical systems, the results presented are sufficient for tracking GEO objects in proximity, when provided to orbit determination software.
The approach allowed consumer/amateur-class, small FOV, COTS equipment to contribute accurate astrometric and photometric data to the PHANTOM ECHOES 2 experiment. This suggests that the application of the technique may increase the utility of COTS equipment and reduce the need for high end/bespoke optical systems in some circumstances. For the MEV-2 case, where determining separation between two sources close in proximity was crucial, images were optimised to prioritise angular resolution over FOV. This study has demonstrated that where such decisions are made to optimise for a certain characteristic (e.g. angular resolution, in this case) it is still possible to retain modest capability for other applications (e.g. astrometry and orbit determination).

More generally, this study has again demonstrated that moderately inexpensive equipment could support a distributed network of SDA sensors and allows for an understanding of the trade-space when determining the right mix of sensors for future systems.

7. ACKNOWLEDGEMENTS

The Authors gratefully acknowledge the data provided by the ARGUS project, including contributions from Trevor Gainey, Bob Trevan and David Wright of the Basingstoke Astronomical Society.

8. REFERENCES

[1] Abdurro'uf et al., The Seventeenth Data Release of the Sloan Digital Sky Surveys: Complete Release of MaNGA, MaStar, and APOGEE-2 Data, The Astrophysical Journal Supplement Series, 259, 2, 2022
[2] MF Skrutskie et al., The Two Micron All Sky Survey (2MASS), The Astronomical Journal 131, 1163 – 1183, 2006
[3] D Lang, DW Hogg, K Mierle, M Blanton, S Roweis, Astrometry.net: Blind astrometric calibration of arbitrary astronomical images, The Astronomical Journal 139, 1782–1800. 2010
[4] AGA Brown et al., Gaia Data Release 2: Summary of the contents and survey properties, 2018, Astronomy & Astrophysics, 616, A1, 2018.

[5] S George, A Ash, T Bessell, J Frith, L Scott, J Skuljan, R Furfaro, V Reddy, PHANTOM ECHOES: A Five-Eyes SDA Experiment to Examine GEO Rendezvous and Proximity Operations, Proceedings of AMOS Conference, 2020.
[6] S George, A Agathanggelou, G Privett, P Halpin, W Feline, A Ash, P Chote, L Scott, J Skuljan, J Alvino, J Frith, PHANTOM ECHOES 2: A Five-Eyes SDA Experiment on GEO Proximity Operations, Proceedings of AMOS Conference, 2021
[7] W Feline, G Privett, A Ash, N Harwood, J Symons, J Davis, Argus: A UK citizen science study in support of the surveillance of space, Proceedings of AMOS Conference, Maui, 2019
[8] G Privett, S George, A Ash, W Feline, G Routledge, An Autonomous Data Reduction Pipeline for Wide Angle EO Systems,, Proceedings of AMOS Conference, Maui, 2017
[9] CD Kuglin, DC Hines, The Phase Correlation Image Alignment Method. Proceeding of IEEE International Conference on Cybernetics and Society, pp. 163-165, New York, 1975
[10] GJ Privett, PJ Kent, Automated Image Registration with ARACHNID, Proc. SPIE 5809, Signal Processing, Sensor Fusion, and Target Recognition, XIV, 2005
[11] BS Reddy, BN Chatterji, An FFT-based technique for translation, rotation and scale-invariant image registration, IEEE Transactions on Image Processing, 5, 1266-1271, 1996
[12] T Matej, C Gohlke, imreg_dft, https://github.com/matejak/imreg_dft, accessed 5 August 2022.